

1 Elevated $p\text{CO}_2$ causes developmental delay in early larval Pacific oysters, *Crassostrea*
2 *gigas*

3

4 Emma Timmins-Schiffman¹, Michael J. O'Donnell², Carolyn S. Friedman¹, and Steven B.
5 Roberts^{1*}

6 ¹ University of Washington, School of Aquatic and Fishery Sciences, Box 355020,
7 Seattle, WA 98195

8 ² University of Washington, Friday Harbor Laboratories, 620 University Rd., Friday
9 Harbor, WA 98250

10

11 *Corresponding author: sr320@uw.edu

12 tel.: (206) 685-3742

13 fax: (206) 685-7471

14

15

16

17

18

19

20

21

22

23

24

25

26

27

28

29

30

31

32

33

34

35

36

37

38

39

40 ABSTRACT

41 Increasing atmospheric CO₂ equilibrates with surface seawater, elevating the
42 concentration of aqueous hydrogen ions. This process, ocean acidification, is a future
43 and contemporary concern for aquatic organisms, causing failures in Pacific oyster
44 (*Crassostrea gigas*) aquaculture. This experiment determines the effect of elevated
45 pCO₂ on the early development of *C. gigas* larvae from a wild Pacific Northwest
46 population. Adults were collected from Friday Harbor, Washington, USA (48°31.7' N,
47 12°1.1' W) and spawned in July 2011. Larvae were exposed to Ambient (400 µatm CO₂),
48 MidCO₂ (700 µatm), or HighCO₂ (1000 µatm). After 24 hours, a greater proportion of
49 larvae in the HighCO₂ treatment were calcified as compared to Ambient. This
50 unexpected observation is attributed to increased metabolic rate coupled with sufficient
51 energy resources. Oyster larvae raised at HighCO₂ showed evidence of a
52 developmental delay by 3 days post-fertilization, which resulted in smaller larvae that
53 were less calcified.

54
55
56
57
58
59
60
61
62
63
64
65
66
67
68
69
70
71
72
73
74
75
76
77
78

79 INTRODUCTION

80 Ocean acidification is expected to affect ecosystems at an accelerating pace
81 over the next century (Caldeira and Wickett 2003; IPCC 2007). Seawater pH declines
82 (acidifies) in association with the uptake of anthropogenic CO₂ and resultant increased
83 H⁺ ion concentration. Projected changes in atmospheric pCO₂ may have significant
84 consequences for natural populations ranging from physiological changes to broad-scale
85 range shifts (Talmage and Gobler 2011; O'Donnell *et al.* 2009; Wong *et al.* 2011;
86 Tomanek *et al.* 2011; Banks *et al.* 2010; Perry *et al.* 2005).

87 Acidification of nearshore waters can occur via a variety of processes, including
88 equilibration with elevated pCO₂ in the atmosphere, upwelling events, terrestrial run-off
89 and respiration. The upper ocean acidification in the North Pacific is proportional to the
90 anthropogenic increase in atmospheric CO₂, enforcing that the present-day pH changes
91 are outside the range of natural variability (Byrne, RH *et al.* 2010). In addition to
92 atmospheric sources of CO₂, oceanic upwelling and nearshore respiration further reduce
93 the pH of water in which larvae develop (as low as pH 7.4 along the west coast of North
94 America) and increasingly result in waters undersaturated with respect to aragonite
95 (Feely *et al.* 2008, 2010). During the spring and summer off the U.S. west coast,
96 upwelling of waters rich in CO₂ and respiration from nearshore biological activity can
97 cause undersaturation of nearshore waters (Feely *et al.* 2008, 2010; Fassbender *et al.*
98 2011). These contemporary processes occur in the same area where planktonic
99 invertebrate larvae congregate. As CO₂ emissions continue to equilibrate with ocean
100 surface water, these habitats that already experience low pH could see further and more
101 sustained increases in pCO₂.

102 Numerous studies have examined developmental consequences of ocean
103 acidification on marine bivalve larvae. Exposure to low pH water early in development
104 caused decreased mid-stage growth and survival in *C. gigas* (Barton *et al.* 2012). *C.*
105 *gigas*'s congener, *C. virginica*, grew more slowly and incorporated less CaCO₃ into their
106 shells at elevated pCO₂ when compared to controls (Miller *et al.* 2009). Similarly, ocean
107 acidification conditions decreased both shell integrity and tissue mass in larval mussels,
108 *Mytilus californianus* (Gaylord *et al.* 2011). Larval Sydney rock oysters (*Saccostrea*
109 *glomerata*) demonstrated reduced survival and slower growth and development when
110 reared under conditions simulating future oceanic pCO₂ (Watson *et al.* 2009). Both clam
111 (*Mercenaria mercenaria*) and scallop larvae (*Argopectens irradians*) were impacted by
112 elevated pCO₂ in their metamorphosis, growth, and lipid synthesis (Talmage and Gobler
113 2011). The effects of ocean acidification have been studied on populations of *C. gigas*
114 from Japan (Kurihara *et al.* 2007), Australia (Parker *et al.* 2010, 2012), and Europe
115 (Gazeau *et al.* 2011), but few studies to date look at these effects on populations of *C.*
116 *gigas* from the United States. Due to differences in experimental design, it is difficult to
117 directly compare the three aforementioned studies, but overall *C. gigas* larvae are

118 smaller when raised at elevated $p\text{CO}_2$ (Kurihara *et al.* 2007; Parker *et al.* 2010; Gazeau
119 *et al.* 2011), demonstrate a developmental delay (Kurihara *et al.* 2007), and have
120 morphological and shell deformities (Kurihara *et al.* 2007; Parker *et al.* 2010; Gazeau *et*
121 *al.* 2011).

122 Pacific oyster larvae are planktotrophs, spending an extended period of one to
123 three weeks in the plankton, where they undergo a variety of important morphological
124 and physiological changes (Strathmann 1985). These developmental changes are
125 frequently associated with environmental cues (Bonar *et al.* 1990) and their successful
126 completion is necessary for larval metamorphosis into a settled juvenile oyster.
127 Organismal responses to ocean acidification vary among and within taxa suggesting that
128 ecological and evolutionary history may influence responses to ocean acidification.
129 Thus, empirical studies are needed to understand the mechanistic responses of species
130 to a specific environmental stress and how the stress corresponds to the species' or
131 population's original ecological niche.

132 One of the primary means by which marine organisms are directly influenced by
133 ocean acidification is through relative concentrations of H^+ and associated decreased
134 availability of CO_3^{2-} . These changes in water chemistry impact calcifying organisms as
135 they rely on CO_3^{2-} to form and maintain carbonate-based structures (Beniash *et al.* 2010;
136 Thomsen and Melzner 2010), while greater H^+ concentration can cause acidosis of body
137 fluids. Acidosis can result in dissolution of calcium carbonate structures, reducing shell
138 thickness and releasing ions into the hemolymph. Many adult aquatic invertebrates can
139 make use of dissolved calcified structures, or possibly actively dissolve their shell, to
140 make HCO_3^- more available as a buffer against internal acidosis. Excess HCO_3^- for
141 buffering can also be acquired from the aquatic environment. This phenomenon has
142 been observed in Dungeness crabs *Cancer magister* (Pane and Barry 2007), blue crabs
143 *Callinectes sapidus* (Henry *et al.* 1981), limpets *Patella vulgata* (Marchant *et al.* 2010)
144 and urchins *Psammechinus miliaris* (Miles *et al.* 2007); however, internal acidosis was
145 not successfully avoided in oysters, *C. gigas* (Lannig *et al.* 2010). It is not clear to what
146 degree larvae can utilize this mechanism to maintain homeostasis under elevated $p\text{CO}_2$
147 conditions, but some invertebrates that inhabit naturally CO_2 -rich environments are able
148 to reproduce and the larvae settle without apparent adverse effects (Thomsen *et al.*
149 2010).

150 Sustained environmental change, such as ocean acidification, can negatively
151 affect both the ecosystem and economy. Shellfish, including oysters, provide important
152 ecosystem services such as improved water quality and benthic-pelagic coupling
153 through the filtration of large volumes of water, release of feces to the benthos, and
154 creation of habitat via reef formation (Coen and Luckenbach 2000). In addition to their
155 ecological roles, molluscs are economically important to many coastal communities
156 worldwide. In 2008, molluscs comprised 64.1% (or 13.1 million tons) of worldwide

157 aquaculture production, with oysters accounting for 31.8% of the total production (FAO
158 2010). The global economic cost of ocean acidification to the mollusc fishery is unclear
159 but has been estimated to increase with rising atmospheric CO₂ levels and terrestrial
160 sources of acidification (Narita *et al.* 2012). Recently, in the Pacific Northwest of the
161 U.S., concern has heightened over the already apparent effects of corrosive, acidified
162 water on both natural and hatchery production of *C. gigas* larvae (Elston *et al.* 2008;
163 Feely *et al.* 2010; Barton *et al.* 2012). Hatchery water supply comes from adjacent
164 natural bays and when upwelling events occur, the water that enters the hatchery can
165 reach *p*CO₂ near 1000 μatm (S. Alin, unpublished data; B. Eudeline, pers. comm.).
166 These upwelling events have been linked to mortality episodes in the hatchery, perhaps
167 due to a combination of acidic water and pathogens associated with the water masses
168 (Elston *et al.* 2008). Acidification events are projected to become more frequent and
169 sustained as atmospheric *p*CO₂ continues to rise.

170 This study characterized the effects of two elevated levels of *p*CO₂ on size,
171 calcification and development during early larval stages of the Pacific oyster,
172 *Crassostrea gigas*. Oyster larvae were raised in two elevated levels of *p*CO₂ (700 and
173 1000 μatm) and ambient (400 μatm) seawater through 72 hours following fertilization.
174 The chemistry scenarios simulated in this study are based on projections for the coming
175 century, but these values of low pH and Ω are already occurring with increasing
176 frequency in nearshore upwelling systems off the U.S. West coast (Feely *et al.* 2010;
177 Hauri *et al.* 2009).

178

179 MATERIAL AND METHODS

180 Seawater chemistry manipulation

181 Experimental conditions were maintained using a flow-through seawater system
182 in Friday Harbor, Washington, USA. Water entering the system was filtered (to 0.2-μm),
183 UV sterilized, and CO₂-depleted using membrane contactors (Membrana, Charlotte,
184 North Carolina, USA) under partial vacuum. Three experimental treatments were
185 chosen to correspond with dissolved CO₂ levels of 400, 700 or 1000 ppm in the
186 atmosphere. These three treatments will be referred to throughout the manuscript as
187 Ambient, MidCO₂, and HighCO₂. Set-point pH levels were determined with the program
188 CO₂SYS (Robbins *et al.* 2010) using an average total alkalinity of 2060 μmol kg⁻¹ based
189 on total alkalinity measurements taken the week prior to the experimental trial.

190 Larval *C. gigas* were held in 3-L microcosms within a large reservoir filled with
191 the respective treatment water. Ambient air stripped of CO₂ by a CO₂ adsorption unit
192 (Twin Tower Engineering, Broomfield, Colorado, USA) was used to aerate the seawater
193 within the reservoirs through a Venturi injector into the larger reservoir of treatment
194 water. This replaced oxygen lost through the degassing process. Reservoir pH was
195 continuously monitored by a Durafet III pH probe (Honeywell, Morristown, New Jersey,

196 USA). When the probe registered that the treatment's pH strayed from its set point, a
197 solenoid would open or close to allow more or less pure CO₂ (Praxair, Danbury,
198 Connecticut, USA) to be injected via the Venturi. The Durafet probe information was fed
199 into a Honeywell UDA2182 pH controller, which also controlled the solenoids.

200 Seawater was pumped from the reservoir into larval microcosms through
201 irrigation drippers (DIG Industries, Sun Valley, California, USA) at a rate of 1.9-L h⁻¹. An
202 outflow tube at the top of the microcosms fitted with 35- μ m mesh allowed water to exit
203 the microcosms while retaining larvae. All systems were equilibrated to the correct
204 treatment level 48 hours prior to the start of the experiment. Water temperature was held
205 at 20.4°C \pm 0.4°C

206

207 Oysters

208 Ten female and four male adult *C. gigas* were collected from Argyle Creek in
209 Friday Harbor, Washington in July 2011. Oysters were strip-spawned into Ambient
210 seawater with eggs and sperm pooled separately (day 0). Pooled eggs (approximately 2
211 million) were divided equally into 18 7.5-cm diameter containers. Sperm was diluted (so
212 as to approximate a 1:1 sperm:egg ratio) in Ambient seawater and added to each
213 container of eggs. After the addition of sperm, the eggs were gently agitated and
214 incubated for 15 minutes to allow for fertilization.

215 Six containers of fertilized eggs were transferred to microcosms containing one
216 of three treatment conditions. Initial densities post-hatching were approximately 1 larva
217 mL⁻¹. On days 1 and 3 post-fertilization, larvae were randomly sampled to determine
218 survival, size, developmental stage, and presence or absence of calcification. For each
219 microcosm sampled, larvae were filtered onto 35- μ m mesh screens and washed with the
220 appropriate seawater. Approximately 100 larvae were removed for each sample,
221 relaxed with 7.5% MgCl₂ and fixed in 4% paraformaldehyde buffered in filtered seawater.
222 The remaining larvae were returned to cleaned microcosms filled with new seawater.
223 Larvae were fed *Dunaliellia* sp. and *Isochrysis* sp. at concentrations of 30,000 cells mL⁻¹
224 each (concentrations for optimal larval growth) on day 2. During feeding, water flow was
225 turned off in microcosms for two hours. All microcosms were cleaned at each sampling
226 event.

227 Larvae were examined using light microscopy to determine survival, size,
228 developmental stage and shell presence/absence. Survival was determined at 20-40x:
229 larvae were counted as dead if there was a complete absence of ciliary movement.
230 Larval hinge length and shell height were measured at 10x magnification with a Nikon
231 Eclipse E600 and NIS Elements Basic Research software (Nikon, Tokyo, Japan). Larval
232 developmental stage and shell presence were determined at 20x magnification using an
233 inverted microscope and double polarized light. Larvae were scored as calcified on day
234 1 post-fertilization if calcified shell was observed at the hinge (Figure 1A). On day 3

235 post-fertilization, larvae were classified as fully calcified if polarized light produced a
236 “Maltese cross” in the larval shell (Figure 1B; LaBarbera 1974).

237

238 Carbonate chemistry

239 Salinity was measured with a conductivity meter (Hach sensION5; Loveland,
240 Colorado, USA) and temperature was measured using a Fluke 1523 thermometer
241 (Fluke, Everett, Washington, USA). Seawater pH entering the microcosms was
242 measured daily using the spectrophotometric (spec) technique outlined in SOP 6b by
243 Dickson *et al.* (2007) to confirm pH measurements from the Durafet probe. When any
244 discrepancies were observed, the Durafet probe was recalibrated. Seawater pH
245 measurements were taken from two microcosms per treatment on days 0, 1, and 3.
246 Final pH values reported here have been corrected for dye addition and temperature.
247 Total alkalinity (A_T) was measured following the open cell titration of SOP 3b (Dickson *et al.*
248 *et al.* 2007). Samples for A_T were taken from incoming water and from two microcosms in
249 each treatment on days 0, 2, and 3. CO₂SYS (Robbins *et al.* 2010) was used to
250 calculate calcium carbonate saturation state (Ω) of aragonite and calcite, carbonate ion
251 concentration, and $p\text{CO}_2$ with A_T and pH as inputs using the following constants: Lueker
252 *et al.* (2000) for CO₂ Constants, Dickson (1990b) for KHSO₄, Total scale (mol kg⁻¹ SW)
253 for pH scale, and Wanninkhof (1992) for Air-Sea Flux.

254

255 Statistics

256 Differences in larval size and mortality across treatments were examined using a
257 two-way ANOVA with fixed effects of treatment and day followed by Tukey’s Honestly
258 Significant Difference test (Tukey’s HSD). A one-way ANOVA was also used to test for
259 differences in larval size among treatments using the combined fixed factor of day-
260 treatment. Larval calcification and developmental stage were compared among
261 treatments using a generalized linear model (GLM). Binomial error distributions were
262 used for GLM analyses. The occurrence of a developmental delay was assessed by
263 fitting the regression of shell height on hinge length to a linear model and testing for
264 differences in the slopes of these lines across treatments. Developmental delay would
265 be demonstrated if the larvae maintained the same allometry across treatments (the
266 slopes of the lines were the same) but were different in size. At least two replicates
267 within treatments and time points were used for all statistical analyses. All analyses
268 were performed in R (R Development Core Team 2011).

269

270 RESULTS

271 Carbonate chemistry

272 Throughout the experiment seawater pH differed across treatments and A_T
273 varied slightly but to the same degree across treatments (Table 1). Mean seawater pH

274 was consistent within but varied among treatments (Figure 2). Mean pH (\pm standard
275 deviation), as measured by the Durafet pH probes (Figure 2) was 7.99 ± 0.04 in the
276 Ambient treatment, 7.75 ± 0.06 in the MidCO₂ treatment and 7.66 ± 0.09 in the HighCO₂
277 treatment. Aragonite and calcite saturation states were greater than 1.0 for the duration
278 of the experiment, except in the HighCO₂ treatment on days 1 and 2 (Table 1).
279 Carbonate ion concentration was lowest in the HighCO₂ treatment (average \pm SD of
280 $61.15 \pm 4.05 \mu\text{mol kg}^{-1}$ seawater, N = 4, Table 1), intermediate in MidCO₂ (74.05 ± 6.43
281 $\mu\text{mol kg}^{-1}$, N = 4), and highest in the Ambient treatment ($120.24 \pm 11.52 \mu\text{mol kg}^{-1}$, N =
282 4). Partial pressure of CO₂ in the seawater averaged $468 \pm 63 \mu\text{atm}$ in the Ambient
283 treatment, $847 \pm 67 \mu\text{atm}$ in the MidCO₂ treatment, and $1065 \pm 58 \mu\text{atm}$ in the HighCO₂
284 treatment.

285

286 Size, development, and calcification

287 Survival was near 100% in all treatments on day 1 (Ambient = 99.0%, MidCO₂
288 and HighCO₂ = 99.7%). On day 3, survival was 92.9% in the Ambient treatment, and
289 was approximately 88.6% in the MidCO₂ and 85.6% in the HighCO₂ treatment. Mortality
290 was similar across treatments (F=0.59, P > 0.05) but different across days (F=17.7, P <
291 0.05).

292 On day 1, a slightly greater proportion (0.977) of larvae at HighCO₂ were at the
293 D-hinge stage (compared to those that were still trocophores), but this difference was
294 not significant (z-value=1.016, P = 0.310; data not shown). The proportion of larvae at
295 the D-hinge stage on day 1 in the Ambient treatment was 0.875 and in MidCO₂ was
296 0.833. Amount of larvae with shell was significantly different among treatments for days
297 1 and 3 post-fertilization. Following 24 hours of treatment (day 1) the proportion of
298 larvae with shell present was inversely proportional to pCO₂ level with the greatest
299 number of larvae with shell in the HighCO₂ treatment (z-value = 2.084, P = 0.0372,
300 Figure 6). On day 3, fewer larvae at HighCO₂ conditions had full shell compared to the
301 other two treatments (z-value = -3.203, P = 0.00136).

302 Larval size (shell height and hinge length) was similar across experimental
303 treatments after 24 hours, however by day 3 larvae grew significantly larger (height and
304 length) in the Ambient and MidCO₂ as compared to the HighCO₂ treatment (Table 2,
305 Figures 3 and 4). Between days 1 and 3 larvae increased in size under Ambient
306 conditions (shell height, P < 1e-7) and MidCO₂ conditions (shell height and hinge length,
307 P < 1e-7 and P = 7.4e-6, respectively; Figures 3 and 4), but did not significantly increase
308 in size under HighCO₂ conditions. By day 3, all larvae observed across treatments were
309 at the D-hinge stage. The slope of the linear regression through shell height versus
310 hinge length for the larvae raised at Ambient pCO₂ was 0.6459 (Figure 5), which was not
311 significantly different from the slope of the regression line through the MidCO₂ data
312 (0.8583, P > 0.05) or from the line through the HighCO₂ size data (0.3625, P > 0.10).

313

314 DISCUSSION

315 Oyster larvae raised at HighCO₂ showed evidence of a developmental delay by 3
316 days post-fertilization, which caused them to be smaller and have less calcified material
317 than controls. These results are consistent with other studies of *Crassostrea* spp. larvae
318 in which elevated pCO₂ resulted in decreased growth and shell mineralization (Kurihara
319 *et al.* 2007; Miller *et al.* 2009). Kurihara *et al.* (2007) raised *C. gigas* to 48 hours post-
320 fertilization at an elevated pCO₂ of about 2268 µatm, much higher than pCO₂ projected
321 for the coming century, and observed a negative effect on calcification as early as 24
322 hours post-fertilization. The authors also observed a developmental delay in reaching
323 the D-hinge stage at 48 hours post-fertilization (Kurihara *et al.* 2007). Since we did not
324 measure growth or calcification in our larvae at 48 hours post-fertilization, we are not
325 able to draw direct comparisons with this time point, but we did observe a developmental
326 delay by 72 hours post-fertilization. Similarly, *Crassostrea virginica* larvae raised from
327 72 hours post-fertilization through competency at different pCO₂ grew more slowly at
328 elevated pCO₂ (560 and 800 µatm) and biomineralized less CaCO₃ than controls;
329 however *Crassostrea ariakensis* showed no effect of pCO₂ treatment (Miller *et al.* 2009).
330 It is likely the observed differences between the studies are related to the much higher
331 pCO₂ level used by Kurihara *et al.* (2007) and species- and population-specific
332 differences in acclimation to ocean acidification

333 The developmental delay is evidenced by similar growth trajectories across
334 treatments (Figure 5) coupled with the smaller size of larvae in the HighCO₂ treatment.
335 This suggests that change in size is not a direct effect of ocean acidification on shell
336 growth and maintenance. In a study comparing faster growing hybrid *C. gigas* larvae to
337 slower growing inbred larvae, slower growth was attributed to reduced feeding rate and
338 differing allocation of internal energy reserves for metabolic processes (Pace *et al.*
339 2006). The stress of elevated pCO₂ can induce similar physiological changes via effects
340 on metabolic demands, resulting in a developmentally delayed phenotype (Stumpp *et al.*
341 2011a). It is difficult to detect developmental delay with complete confidence in studies
342 that do not follow larvae through to settlement. In one such study, larval
343 *Strongylocentrotus purpuratus* were exposed to elevated pCO₂ throughout their larval
344 period and from this perspective it was apparent that ocean acidification caused a delay
345 in development, although at discrete time points this delay could be interpreted as
346 overall smaller size (Stumpp *et al.* 2011a). Developmental delay may give these species
347 the energetic resources they need to survive stress and reach the later developmental
348 stages of metamorphosis and settlement. However, a delay in development opens the
349 possibility for a host of other complications for pelagic larvae, such as greater potential
350 to be advected to unsuitable habitat (Strathmann 1985), greater chance of being
351 exposed to predators (Underwood and Fairweather 1989), and an overall longer time in

352 the water column where environmental conditions are variable and risky for a free-
353 floating larva.

354 A greater percentage of the larvae in the HighCO₂ treatment had shell present by
355 24 hours fertilization compared to both Ambient and MidCO₂. The impact of ocean
356 acidification on larval invertebrates can change in direction and magnitude as the larvae
357 switch from a non-feeding to a feeding stage. The larvae at HighCO₂ were most likely
358 able to maintain a normal development rate and calcified structures early in
359 developmental because an increased metabolic rate would have been supported by
360 sufficient maternal energy resources. In early development, *C. gigas* depend on
361 maternal lipid reserves, but after 24 hours in the plankton, the larvae become dependent
362 upon external resources (Gallager *et al.* 1986). Environmental stress frequently
363 instigates an elevated metabolic rate (Lannig *et al.* 2010; Stumpp *et al.* 2011a). During
364 the non-feeding stage, larvae may have enough maternal resources to support their
365 increased metabolic rate and sustain normal or even accelerated growth and
366 development. In the non-feeding lecithotrophic larvae of the common sun star
367 (*Crossaster papposus*), larvae at low pH developed and grew faster than those in
368 ambient conditions (Dupont *et al.* 2010). Once the metabolic switch to external
369 resources occurs, the larvae may not be able to get enough resources to sustain the
370 increased metabolic rate as well as normal development. A similar trend is seen in
371 larval purple sea urchins, *Strongylocentrotus purpuratus*. Ocean acidification had a
372 larger impact on the feeding larval stage of *S. purpuratus* than it did on the non-feeding
373 stage (Stumpp *et al.* 2011a). Similarly to *C. gigas*, *S. purpuratus* demonstrated a
374 developmental delay starting with the onset of feeding (Stumpp *et al.* 2011a). At the
375 same time, routine metabolic rate increased in both elevated pCO₂ and ambient
376 treatment, but increased more at low pH (Stumpp *et al.* 2011a). The results from these
377 studies suggest that the maintenance of homeostasis becomes more difficult under the
378 energetic demands of ocean acidification stress; however, the physiological stress is
379 realized as developmental delay, with associated phenotypes of less shell and smaller
380 size, only when larvae are in a feeding stage. Reallocation of resources associated with
381 invertebrate responses to ocean acidification has been shown to affect several
382 processes, including as soft tissue growth (Gaylord *et al.* 2011; Beniash *et al.* 2010),
383 scope for growth (Stumpp *et al.* 2011a), and shell integrity (Gaylord *et al.* 2011; Melzner
384 *et al.* 2011).

385 Larval shell formation is closely linked to development and begins by 24 hours
386 post-fertilization. Numerous species experience decreased calcification when water is
387 undersaturated with respect to aragonite (Kurihara *et al.* 2007; Miller *et al.* 2009; Crim *et al.*
388 2011; Gazeau *et al.* 2011; Byrne, M. *et al.* 2010), although some species are still able
389 to form apparently normal calcified structures in undersaturated conditions (Dupont *et al.*
390 2010; Catarino *et al.* 2011; Yu *et al.* 2011). Early *C. gigas* larval shells are made of

391 amorphous calcium carbonate and aragonite (Weiss *et al.* 2002), two of the more
392 soluble forms of CaCO₃ at low pH. Invertebrates are able to control calcification through
393 amorphous mineral precursors and metabolites (Weiss 2011), thus decreasing the
394 potential effects of a corrosive environment. On days 1 and 2, Ω_{Ar} was below 1.0,
395 causing the seawater to be undersaturated with respect to aragonite. Calcification can
396 become energetically costly due to scarcity of CO₃²⁻ ions in the environment and
397 disruption of ionic gradients of the calcifying compartment from changes in H⁺. If oyster
398 larvae remove a fixed number of H⁺ from their calcifying fluid versus maintaining a fixed
399 ratio of extracellular:intracellular H⁺, then their energy budget would be more taxed
400 during environmental hypercapnia (Ries 2011). This added stress on the process of
401 calcification could have contributed to the energy budget shifts that led to a
402 developmental delay.

403 In this study, *C. gigas* tolerated the MidCO₂ treatment through 3 days post-
404 fertilization. The lack of negative effects on shell formation and maintenance in the
405 larvae from the MidCO₂ treatment suggests that a cut-off of $\Omega_{Ar} < 1.0$ is significant in
406 terms of the ability of this population to biomineralize at this time point in development. It
407 is also possible that the high level of food available to the larvae modulated the impact of
408 ocean acidification and could have led to an underestimation its effect in this treatment
409 (Melzner *et al.* 2011). An elevated $p\text{CO}_2$ of 750 ppm (Ω_{Ar} of about 1.0) had significant
410 negative effects on hard clam (*Mercenaria mercenaria*) and bay scallop (*Argopecten*
411 *irradians*) larvae after about 3 weeks of exposure as evidenced by decreased survival,
412 development, growth and lipid synthesis (Talmage and Gobler 2011). The comparable
413 exposure conditions in our study (MidCO₂) did not have a negative impact over the time
414 period observed. Due to the similarities of carbonate chemistry parameters with
415 Talmage and Gobler (2011), the differential responses observed across species are
416 likely indicative of variability in species, developmental stage tolerances, or length of
417 exposure. Longer experiments in larvae have demonstrated that the negative effects of
418 ocean acidification persist and sometimes worsen in mussels *Mytilus californianus*
419 (Gaylord *et al.* 2011), urchins *S. purpuratus* (Stumpp *et al.* 2011 a and b), abalone
420 *Haliotis kamtschatkana* (Crim *et al.* 2011), and oysters *Crassostrea ariakensis* and *C.*
421 *virginica* (Miller *et al.* 2009). The compounding negative effects of ocean acidification
422 during an experiment may be due to a species' decreasing ability to tolerate a specific
423 environmental stress as their metabolic needs change throughout development.

424

425 *Conclusions*

426 In this study we observed that an acute, 72 hour exposure to end-of-century
427 projections of ocean acidification (HighCO₂) has a negative impact on development in
428 oyster larvae. Additionally, this study revealed that moderate changes in seawater
429 chemistry (MidCO₂, about 800 μatm , mean $\Omega_{Ar} > 1.19 \pm 0.10$) did not have an observed

430 significant impact on larvae through 3 days post-fertilization. It appears the effects of an
431 environmental stress, such as ocean acidification, vary depending on developmental and
432 metabolic stage of *C. gigas* larvae. This is most likely directly associated with a switch in
433 larval energy metabolism as the oysters develop from a non-feeding stage to a feeding
434 stage. In order to effectively evaluate the possibility of acclimation or adaptation, future
435 research should focus on characterizing larvae from diverse genotypes and locations as
436 well as assessing any influences that might be experienced later in development.

437

438 ACKNOWLEDGEMENTS

439 We would like to thank Drs. Ken Sebens and Emily Carrington for use of lab
440 space and facilities at Friday Harbor Labs. Support from National Science Foundation
441 grant EF1041213 to Dr. Carrington funded the construction of the ocean acidification
442 system and analytical equipment used in this study. National Oceanographic and
443 Atmospheric Administration Saltonstall-Kennedy Program grant # NA09NMF4270093 to
444 Dr. Steven Roberts and Dr. Carolyn Friedman also supported this research project. Matt
445 George, Laura Newcomb, and Michelle Herko provided help with maintenance of the
446 ocean acidification system, larval care, and water chemistry analysis, respectively.
447 Thank you to Dr. Richard Strathmann for his advice on larval care and to Dr. Billie
448 Swalla for advice on fixation and for use of her lab space. Dr. Brent Vadopalas and Dr.
449 Loveday Conquest were incredibly helpful with advice on statistical analysis. Lisa
450 Crosson, Mackenzie Gavery, Caroline Storer, and Sam White provided valuable, critical
451 feedback during the writing process. We are very appreciative of the thorough and
452 helpful comments from two anonymous reviewers and from the editor of this issue, Dr.
453 Sam Dupont.

454

455 REFERENCES

- 456 Banks SC, Ling SD, Johnson CR, Piggott MP, Williamson JE, Behrgegaray LB (2010)
457 Genetic structure of a recent climate change-driven range extension. *Molecular*
458 *Ecology* 19: 2011-2024
- 459 Barton A, Hales B, Waldbusser G, Langdon C, Feely RA (2012) The Pacific oyster,
460 *Crassostrea gigas*, shows negative correlation to naturally elevated carbon
461 dioxide levels: Implications for near-term ocean acidification impacts. *Limnology*
462 *and Oceanography* 57: 698-710
- 463 Beniash E, Ivanina A, Lieb NS, Kurochkin II, Sokolova IM (2010) Elevated levels of
464 carbon dioxide affects metabolism and shell formation in oysters *Crassostrea*
465 *virginica*. *Marine Ecology Progress Series* 419: 95-108
- 466 Bonar DB, Coon SL, Walch M, Weiner RM, Fitt W (1990) Control of oyster settlement
467 and metamorphosis by endogenous and exogenous chemical cues. *Bulletin of*
468 *Marine Science* 46: 484-498.

469 Byrne M, Ho M, Wong E, Soars NA, Selyakumaraswamy P, Shepard-Brennand H,
470 Dworjanyn SA, David AR (2010). Unshelled abalone and corrupted urchins:
471 development of marine calcifiers in a changing ocean. Proc R Soc B.
472 doi:10.1098/rspb.2010.2404.

473 Byrne RH, Mecking S, Feely RA, Liu X (2010). Direct observations of basin-wide
474 acidification of the North Pacific Ocean. Geophysical Research Letters.
475 doi:10.1029/2009GL040999

476 Caldeira K, Wickett ME (2003) Anthropogenic carbon and ocean pH. Nature 425:365.

477 Catarino AI, De Ridder C, Gonzalez M, Gallardo P, Dubois P (2011) Sea urchin *Arbacia*
478 *dufresnei* (Blainville 1825) larvae response to ocean acidification. Polar Biology.
479 doi: 10.1007/s00300-011-1074-2

480 Coen LD, Luckenbach MW (2000) Developing success criteria and goals for evaluating
481 oyster reef restoration: Ecological function or resource exploitation? Ecological
482 Engineering 15: 323-343

483 Crim RN, Sunday JM, Harley CDG (2011) Elevated seawater CO₂ concentrations impair
484 larval development and reduce larval survival in endangered northern abalone
485 (*Haliotis kamtschatkana*). Journal of Experimental Marine Biology and Ecology
486 400: 272-277

487 Dickson AG, Sabine CL, Christian JR (2007) Guide to best practices for ocean CO₂
488 measurements. Sidney, British Columbia, North Pacific Marine Science
489 Organization, 176 pp.

490 Dupont S, Lundve B, Thorndyke M (2010) Near future ocean acidification increases
491 growth rate of the lecithotrophic larvae and juveniles of the sea star *Crossaster*
492 *papposus*. J Exp Zool (Mol Dev Evol) 314B: 382-389

493 Elston RA, Hasegawa H, Humphrey KL, Polyak IK, Häse CC (2008) Re-emergence of
494 *Vibrio tubiashii* in bivalve aquaculture: severity, environmental drivers,
495 geographic extent, and management. Dis Aquat Org 82: 119-134

496 FAO Fisheries and Aquaculture Department (2010) World aquaculture 2010. FAO
497 Fisheries and Aquaculture Department. Technical Paper. No. 500/1. Rome, FAO.
498 2011. 105 pp.

499 Fassbender AJ, Sabine CL, Feely RA, Langdon C, Mordy CW (2011) Inorganic carbon
500 dynamics during northern California coastal upwelling. Continental Shelf
501 Research 31: 1180-1192

502 Feely RA, Alin SR, Newton J, Sabine CL, Warner M, Devol A, Krembs C, Maloy C
503 (2010) The combined effects of ocean acidification, mixing, and respiration on pH
504 and carbonate saturation in an urbanized estuary. Estuarine, Coastal and Shelf
505 Science 88: 442-449

506 Feely RA, Sabine CL, Hernandez-Ayon JM, Ianson D, Hales B (2008) Evidence for
507 upwelling of corrosive “acidified” water onto the continental shelf. *Science* 320:
508 1490-1492

509 Gallagher SM, Mann R, Sasaki GC (1986) Lipid as an index of growth and viability in
510 three species of bivalve larvae. *Aquaculture* 56: 81-103

511 Gaylord B, Hill TM, Sanford E, Lenz EA, Jacobs LA, Sato KN, Russell AN, Hettinger A
512 (2011) Functional impacts of ocean acidification in an ecologically critical
513 foundation species. *J Exp Biol* 214: 2586-2594

514 Gazeau F, Gattuso J-P, Greaves M, Elderfield H, Peene J, Heip CHR, Middelburg JJ
515 (2011) Effects of carbonate chemistry alteration on early embryonic development
516 of the Pacific oyster (*Crassostrea gigas*). *PLoS One*
517 doi:10.1371/journal.pone.0023010

518 Hauri C, Gruber N, Plattner G-K, Alin S, Feely RA, Hales B, Wheeler PA (2009) Ocean
519 acidification in the California Current System. *Oceanography* 22: 60-71

520 Henry RP, Kormanik GA, Smatresk NJ, Cameron JN (1981) The role of CaCO_3
521 dissolution as a source of HCO_3^- for the buffering of hypercapnic acidosis in
522 aquatic and terrestrial decapod crustaceans. *J Exp Biol* 94: 269-273.

523 Intergovernmental Panel on Climate Change (IPCC) (2007) Contribution of Working
524 Groups I, II, and III to the Fourth Assessment Report of the Intergovernmental
525 Panel on Climate Change. Pachauri, R.K., Reisinger, A. (Eds.), IPCC, Geneva,
526 Switzerland, pp. 104

527 Kurihara H, Kato S, Ishimatsu A. (2007) Effects of increased seawater pCO_2 on early
528 development of the oysters *Crassostrea gigas*. *Aquatic Biology* 1: 91-98

529 LaBarbera M (1974) Calcification of the first larval shell of *Tridacna squamosa*
530 (*Tridacnidae*: *Bivalvia*). *Mar Biol* 25: 233-238

531 Lannig G, Eilers S, Pörtner HO, Sokolova IM, Bock C (2010) Impact of ocean
532 acidification on energy metabolism of Oyster, *Crassostrea gigas*-Changes in
533 metabolic pathways and thermal response. *Mar Drugs* 8: 2318-2339

534 Marchant HK, Calosi P, Spicer JI (2010) Short-term exposure to hypercapnia does not
535 compromise feeding, acid-base balance or respiration of *Patella vulgata* but
536 surprisingly is accompanied by radula damage. *Journal of the Marine Biological*
537 *Association of the United Kingdom* 90: 1379-1384

538 Melzner F, STange P, Trubenbach K, Thomsen J, Casties I, Panknin U, Gorb SN,
539 Gutowska MA (2011) Food supply and seawater pCO_2 impact calcification and
540 internal shell dissolution in the blue mussel *Mytilus edulis*. *PLoS ONE* 6: e24223.
541 doi:10.1371/journal.pone.0024223

542 Miller AW, Reynolds AC, Sobrino C, Riedel GF (2009) Shellfish face uncertain future in
543 high CO_2 world: Influence of acidification on oyster larvae calcification and growth
544 in estuaries. *PLoS ONE* 4: e5661. doi:10.1371/journal.pone.0005661

545 Miles H, Widdicombe S, Spicer JI, Hall-Spencer J (2007) Effects of anthropogenic
546 seawater acidification on acid-base balance in the sea urchin *Psammechinus*
547 *miliaris*. Marine Pollution Bulletin 54: 89-96

548 Narita D, Rehdanz K, Tol RSJ (2012) Economic costs of ocean acidification: a look into
549 the impacts on global shellfish production. Climatic Change. doi:10.1007/s10584-
550 011-0383-3

551 O'Donnell MJ, Hammond LM, Hofmann GE (2009) Predicted impact of ocean
552 acidification on a marine invertebrate: elevated CO₂ alters response to thermal
553 stress in sea urchin larvae. Mar Biol 156: 439-446

554 Pace DA, Marsh AG, Leong PK, GreenAJ, Hedgecock D, Manahan DT (2006)
555 Physiological bases of energetically determined variation in growth of marine
556 invertebrate larvae: A study of growth heterosis in the bivalve *Crassostrea gigas*.
557 Journal of Experimental Marine Biology and Ecology 335: 188-209.

558 Pane EF, Barry JP (2007) Extracellular acid-base regulation during short-term
559 hypercapnia is effective in a shallow-water crab, but ineffective in a deep-sea
560 crab. Mar Ecol Prog Ser 334: 1-9

561 Parker LM, Ross PM, O'Connor WA (2010) comparing the effect of elevated pCO₂ and
562 temperature on the fertilization and early development of two species of oysters.
563 Mar Biol 157: 2435-2452

564 Parker LM, Ross PM, O'Connor WA, Borysko L, Raftos DA, Portner H-O (2012) Adult
565 exposure influences offspring response to ocean acidification in oysters. Global
566 Change Biology 18: 82-92

567 Perry A, Low PJ, Ellis JR, Reynolds JD (2005) Climate change and distribution shifts in
568 marine fishes. Science 308:1912-1915

569 Ries JB (2011) A physicochemical framework for interpreting the biological calcification
570 response to CO₂-induced ocean acidification. Geochimica et Cosmochimica Acta
571 75: 4053-4064.

572 Robbins LL, Hansen ME, Kleypas JA, Meylan SC (2010) CO₂calc: A User-Friendly
573 Carbon Calculator for Windows, Mac OS X, and iOS (iPhone): U.S. Geological
574 Survey Open File Report 2010-1280, 42pp.

575 Strathmann RR (1985) Feeding and nonfeeding larval development and life-history
576 evolution in marine invertebrates. Ann. Rev. Ecol. Syst. 16: 339-361

577 Stump M, Wren J, Melzner F, Thorndyke MC, Dupont ST (2011a) CO₂ induced
578 seawater acidification impacts sea urchin larval development I: Elevated
579 metabolic rates decrease scope for growth and induce developmental delay
580 Comparative Biochemistry and Physiology – Part A: Molecular and Integrative
581 Physiology 160: 331-340

582 Stump M, Dupont ST, Thorndyke MC, Melzner F (2011b) CO₂ induced seawater
583 acidification impacts sea urchin larval development II: Gene expression patterns

584 in pluteus larvae. Comparative Biochemistry and Physiology – Part A: Molecular
585 and Integrative Physiology 160: 320-330

586 Talmage SC, Gobler CJ (2011) Effects of elevated temperature and carbon dioxide on
587 the growth and survival of larvae and juveniles of three species of northwest
588 Atlantic bivalves. PLoS One doi: 10.1371/journal.pone.0026941

589 Thomsen J, Melzner F (2010) Moderate seawater acidification does not elicit long-term
590 metabolic depression in the blue mussel *Mytilus edulis*. Mar Biol 157: 2667-2676

591 Tomanek L, Zuzow MJ, Ivanina AV, Beniash E, Sokolova IM (2011) Proteomic response
592 to elevated P_{CO2} level in eastern oysters, *Crassostrea virginica*: evidence for
593 oxidative stress. J Exp Biol 214: 1836-1844

594 Underwood AJ, Fairweather PG (1989) Supply-side ecology and benthic marine
595 assemblages. Trends in Ecology and Evolution 4: 16-20

596 Watson S-A, Southgate PC, Tyler PA, Peck LS (2009) Early larval development of the
597 Sydney rock oyster *Saccostrea glomerata* under near-future predictions of CO₂-
598 driven ocean acidification. Journal of Shellfish Research 28: 431-437

599 Weiss IM (2011) Biomaterials: Metabolites empowering minerals. Nature Chemical
600 Biology 7: 192-193.

601 Weiss IM, Tuross N, Addadi L, Weiner S (2002) Mollusc larval shell formation:
602 Amorphous calcium carbonate is a precursor phase for aragonite. J Exp Zool
603 293: 478-491

604 Wong KKW, Lane AC, Leung PTY, Thiyagarajan V (2011) Response of larval barnacle
605 proteome to CO₂-driven seawater acidification. Comparative Biochemistry and
606 Physiology Part D: Genomics and Proteomics 6: 310-321

607 Yu PC, Matson PG, Martz TR, Hofmann GE (2011) The ocean acidification seascape
608 and its relationship to the performance of calcifying marine invertebrates:
609 Laboratory experiments on the development of urchin larvae framed by
610 environmentally-relevant pCO₂/pH. Journal of Experimental Marine Biology and
611 Ecology 400: 288-295

612
613
614
615
616
617
618
619
620
621
622

623 FIGURE LEGENDS

| Treatment | Day | Temperature (°C) | Salinity (ppt) | Total Alkalinity (μmol/kg) | pH (Durafet) | pH (spec) | pCO ₂ (μatm) | Ω (calcite) | Ω (aragonite) | CO ₃ ²⁻ (μmol/kg) |
|---------------------|------|------------------|----------------|----------------------------|--------------|-----------|-------------------------|-------------|---------------|---|
| Ambient | 0 | 20.38 | 28.13 | 1998.72 | 7.95 | 7.90 | 557.22 | 2.62 | 1.67 | 104.27 |
| | 1 | 20.50 | 27.97 | 2005.28 | 7.99 | 7.97 | 466.27 | 2.14 | 1.36 | 120.26 |
| | 2 | 20.49 | 28.16 | 1965.59 | 7.96 | 8.00 | 420.92 | 3.15 | 2.01 | 125.38 |
| | 3 | 20.46 | 28.91 | 2021.96 | 8.00 | 8.00 | 428.43 | 3.27 | 2.10 | 131.03 |
| | μ±SD | 20.46±0.05 | 28.29±0.42 | 1997.89±23.65 | 7.99±0.04 | | 468±63 | | | 120.24±11.52 |
| MidCO ₂ | 0 | 20.00 | 28.13 | 2003.25 | 7.75 | 7.73 | 860.92 | 1.83 | 1.17 | 72.79 |
| | 1 | 20.25 | 27.97 | 1983.64 | 7.73 | 7.75 | 812.40 | 1.90 | 1.21 | 75.48 |
| | 2 | 20.18 | 28.16 | 1969.06 | 7.78 | 7.69 | 935.39 | 1.66 | 1.06 | 66.21 |
| | 3 | 20.14 | 28.91 | 2022.46 | 7.77 | 7.77 | 780.96 | 2.04 | 1.31 | 81.73 |
| | μ±SD | 20.14±0.11 | 28.29±0.42 | 1994.60±23.26 | 7.75±0.06 | | 847±67 | | | 74.05±6.43 |
| HighCO ₂ | 0 | 20.25 | 28.13 | 2001.57 | 7.67 | 7.66 | 1025.33 | 1.59 | 1.02 | 63.28 |
| | 1 | 20.47 | 27.97 | 1979.61 | 7.64 | 7.61 | 1149.99 | 1.42 | 0.91 | 56.46 |
| | 2 | 20.10 | 28.16 | 1966.46 | 7.70 | 7.64 | 1057.36 | 1.49 | 0.95 | 59.30 |
| | 3 | 20.41 | 28.91 | 2023.45 | 7.64 | 7.66 | 1030.70 | 1.64 | 1.05 | 65.54 |
| | μ±SD | 20.31±0.17 | 28.29±0.42 | 1992.77±25.06 | 7.66±0.09 | | 1065±58 | | | 61.15±4.05 |

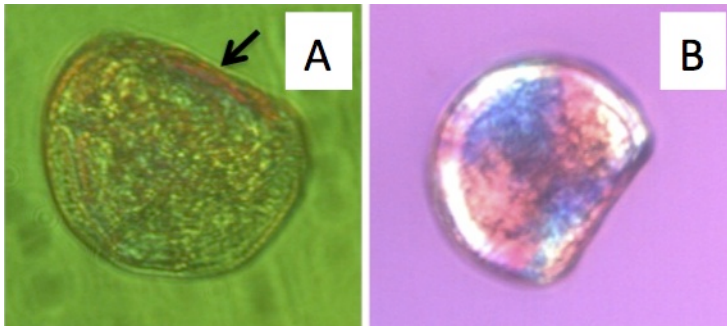
624

625 **Table 1.** Water chemistry data for three experimental treatments – Ambient, MidCO₂,
 626 and HighCO₂. Temperature and Durafet pH measurements are averages from each day
 627 based on the Honeywell controller logs. Salinity, total alkalinity (A_T), and
 628 spectrophotometric (spec) pH are point measurements taken each day. Partial pressure
 629 of CO₂, Ω, and CO₃²⁻ were calculated from spec pH and A_T. Mean and standard
 630 deviation (μ±SD) for the following parameters are given for all 3 days: temperature,
 631 salinity, A_T, pH, pCO₂, and CO₃²⁻.

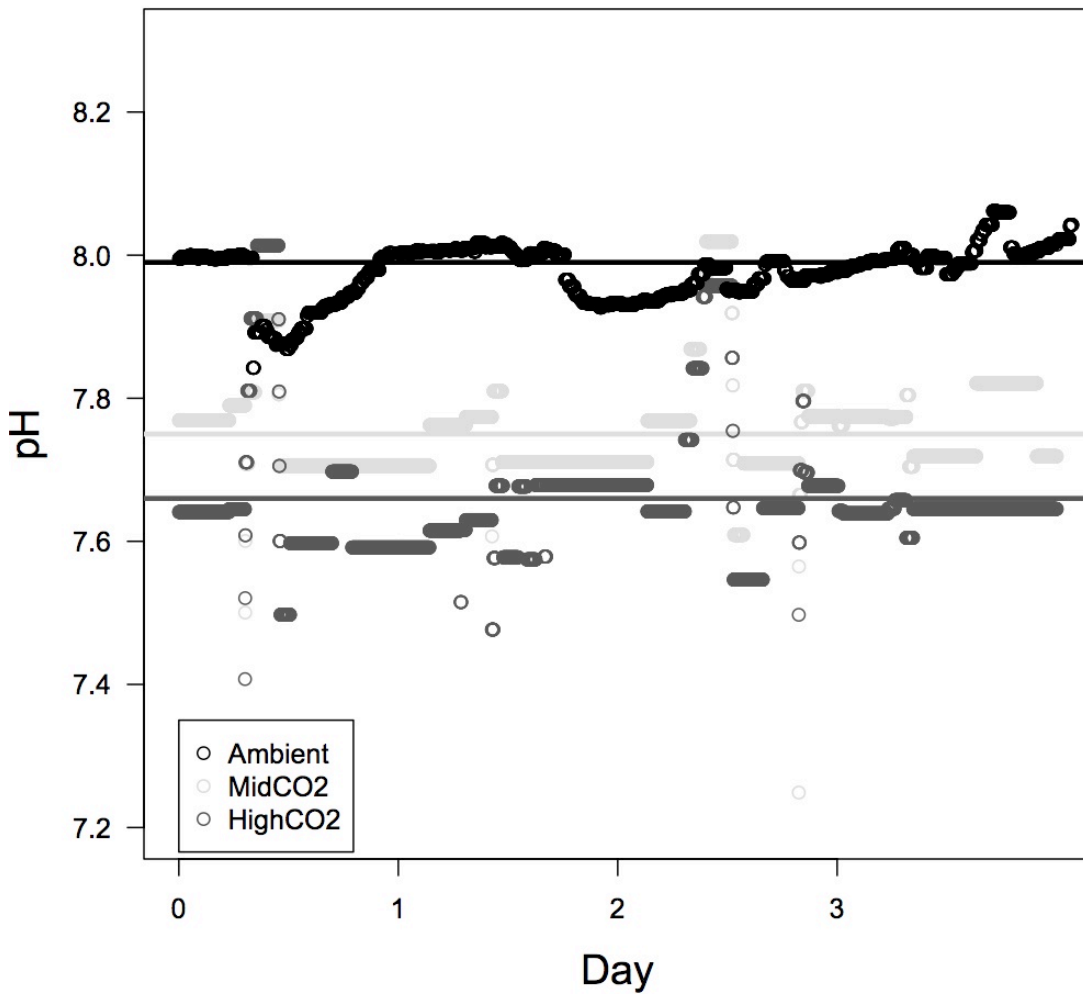
| Treatment | Hinge Length | | Shell Height | |
|--------------------------|--------------------|---------------------|--------------------|---------------------|
| | MidCO ₂ | HighCO ₂ | MidCO ₂ | HighCO ₂ |
| 2-way ANOVA Ambient | 0.250 | 0.0362 | 0.985 | <<0.001 |
| MidCO ₂ | - | <<0.001 | - | <<0.001 |
| 1-way ANOVA Ambient | 0.849 | 0.984 | 0.585 | 0.885 |
| Day 1 MidCO ₂ | - | 0.993 | - | 0.992 |
| 1-way ANOVA Ambient | 0.565 | 0.0311 | 0.261 | <<0.001 |
| Day 3 MidCO ₂ | - | <<0.001 | - | <<0.001 |

632

633 **Table 2.** Results from post-hoc Tukey’s HSD following ANOVA for comparisons of
 634 hinge length and shell height among treatments. The 2-way ANOVA was performed
 635 with “treatment” and “day” as fixed effects and the one-way ANOVA was performed with
 636 the fixed effect of “day-treatment”.

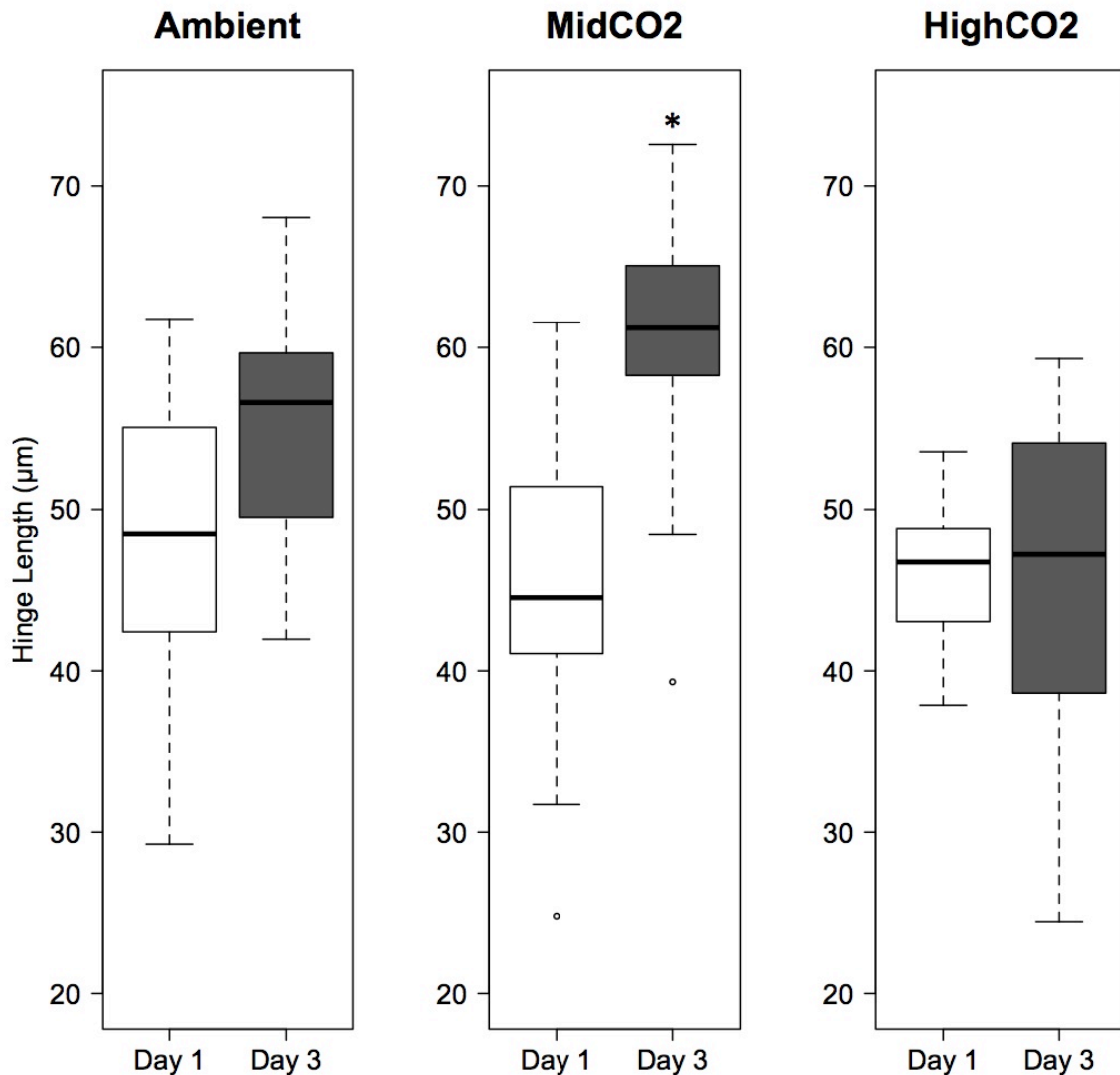


637
 638 **Fig. 1** D-hinge larvae under polarized light portraying calcification at the hinge without a
 639 Maltese cross in the shell (A) and full calcification as evidenced by the Maltese cross
 640 (B).

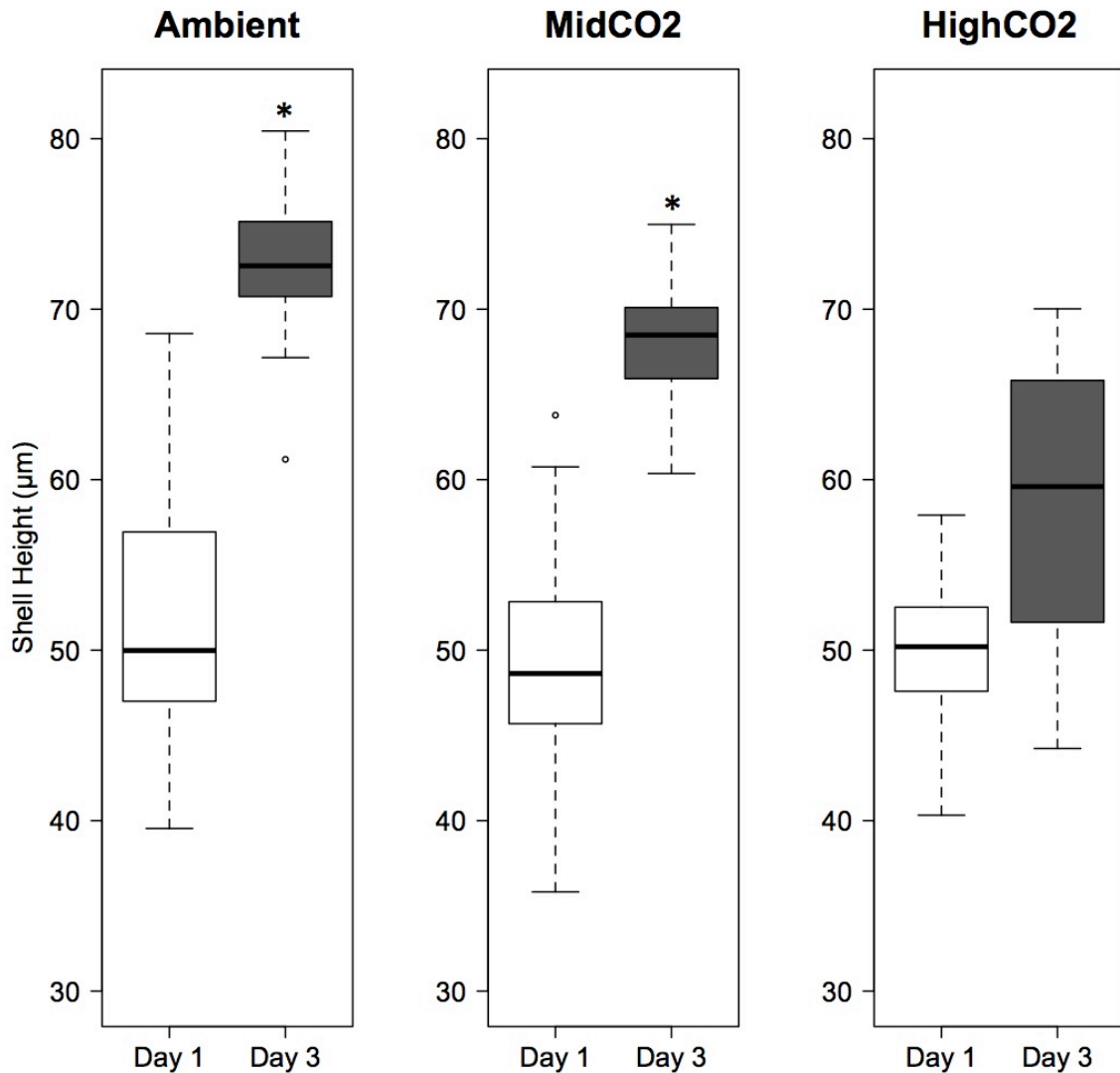


641
 642 **Fig. 2** Profiles of pH measurements in the three different treatments – Ambient (black),
 643 MidCO₂ (light gray), and HighCO₂ (dark gray). Average pH for the experiment for each

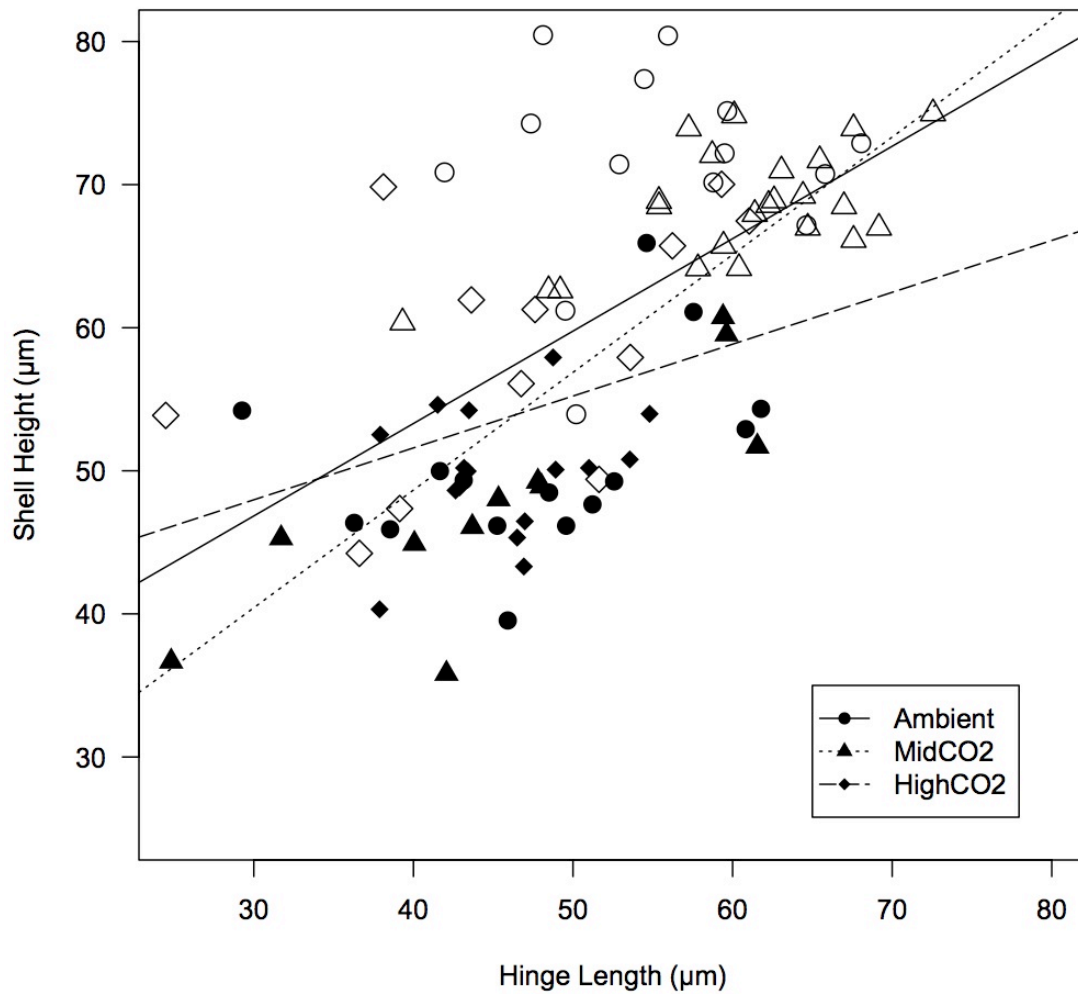
644 treatment is represented by solid lines. The Durafet probes recorded pH measurements
645 every minute.



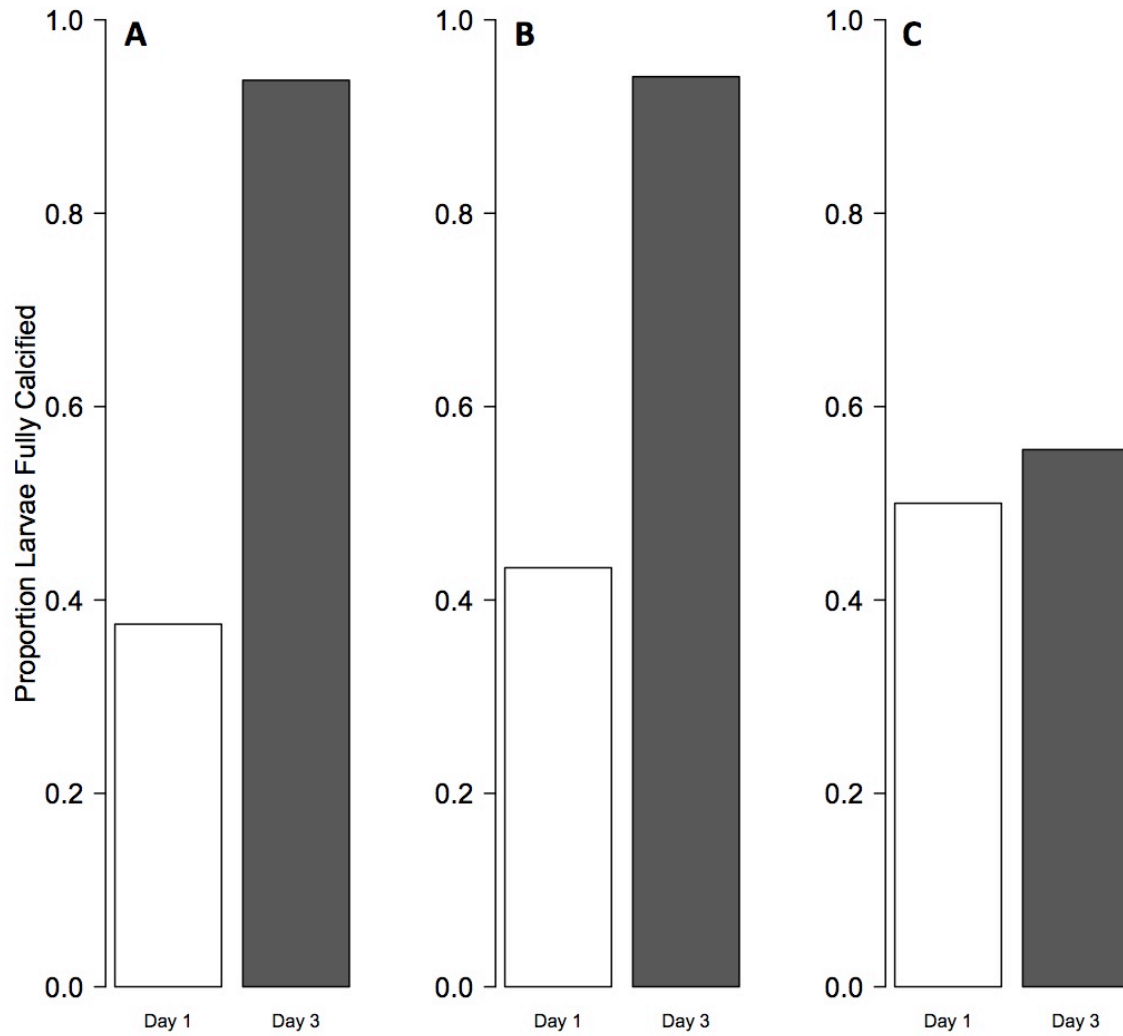
646
647 **Fig. 3** Larval hinge length on day 1 (white boxplots) and day 3 (gray boxplots). Results
648 are shown for the Ambient treatment, MidCO₂ treatment, and HighCO₂ treatment.
649 Boxplots contain the middle 50% of the data and dashed lines encompass data within
650 1.5x the spread of the middle 50%. Open circles represent outliers. Horizontal black
651 bars indicate median values. An asterisk indicates significant differences within a
652 treatment. On day 3, larvae in the HighCO₂ treatment were significantly smaller than
653 those in the other two treatments ($P < 0.05$).



654
 655 **Fig. 4** Larval shell height on day 1 (white boxplots) and day 3 (gray boxplots). Results
 656 are shown for the Ambient treatment, MidCO₂ treatment, and HighCO₂ treatment.
 657 Boxplots contain the middle 50% of the data and dashed lines encompass data within
 658 1.5x the spread of the middle 50%. Open circles represent outliers. Horizontal black
 659 bars indicate median values. An asterisk indicates significant differences within a
 660 treatment. On day 3, shell height was reduced in larvae at HighCO₂ relative to those
 661 raised at Ambient and at MidCO₂ (P < 0.01).



662
 663 **Fig. 5** Regression of larval shell height on hinge length by treatment and day. Data from
 664 larvae raised under Ambient $p\text{CO}_2$ conditions are represented by circles, MidCO₂ are
 665 triangles, and HighCO₂ are diamonds. Size data from day 1 are in black and day 3 are
 666 in white. The solid line is the regression line for the Ambient data (intercept = 27.47,
 667 slope = 0.65), dotted for MidCO₂ (intercept = 15.76, slope = 0.82), and dashed for
 668 HighCO₂ (intercept = 37.10, slope = 0.36). The slopes of all the lines are statistically the
 669 same ($P > 0.05$).



670
 671 **Fig. 6** Proportion of larvae calcified exposed to elevated $p\text{CO}_2$. Bars represent
 672 calcification on day 1 (white) and day 3 (gray). Proportion of larvae calcified are
 673 provided from the Ambient treatment (panel A), MidCO₂ treatment (panel B), and
 674 HighCO₂ treatment (panel C). There is a significant difference in calcification among
 675 treatments, with the highest proportion of larvae calcified at HighCO₂ on day 1 and the
 676 fewest larvae calcified in HighCO₂ on day 3.

677
 678